the plant journal

SEB SOCIETY FOR EXPERIMENTAL BIOLOGY

The Plant Journal (2020) doi: 10.1111/tpj.14922

ZmDREB2A regulates *ZmGH3.2* and *ZmRAFS*, shifting metabolism towards seed aging tolerance over seedling growth

Qinghui Han[1,2], Kelu Chen[1,2], Dong Yan[1,2], Guanglong Hao[1,2], Junlong Qi[1,2], Chunmei Wang[3], Lynnette M.A. Dirk[4], A. Bruce Downie[4], Jianhua Gong[5], Jianhua Wang[5,*] and Tianyong Zhao[1,2,*]

[1]*State Key Laboratory of Crop Stress Biology for Arid Areas, College of Life Sciences, Northwest A&F University, Yangling, Shaanxi 712100, China,*

[2]*The Key Laboratory of Biology and Genetic Improvement of Maize in Arid Areas of the Northwest Region, Ministry of Agriculture, Northwest A&F University, Yangling, Shaanxi 712100, China,*

[3]*The Biology Teaching and Research Core Facility, College of Life Sciences, Northwest A&F University, Yangling, Shaanxi, China,*

[4]*Department of Horticulture, Seed Biology Group, College of Agriculture, Food, and Environment, University of Kentucky, Lexington, KY 40546, USA, and*

[5]*Center of Seed Science and Technology, Beijing Key Laboratory of Crop Genetics and Breeding, Innovation Center for Seed Technology (Ministry of Agriculture), China Agricultural University, Beijing 100094, China*

Received 16 December 2019; revised 1 June 2020; accepted 12 June 2020.
*For correspondence (e-mails tzhao2@nwafu.edu.cn; wangjh63@cau.edu.cn).

SUMMARY

Seed aging tolerance and rapid seedling growth are important agronomic traits for crop production; however, how these traits are controlled at the molecular level remains largely unknown. The unaged seeds of two independent maize *DEHYDRATION-RESPONSIVE ELEMENT-BINDING2A* mutant (*zmdreb2a*) lines, with decreased expression of *GRETCHEN HAGEN3.2* (*ZmGH3.2*, encoding indole-3-acetic acid [IAA] deactivating enzyme), and increased IAA in their embryo, produced longer seedling shoots and roots, than the null segregant (NS) controls. However, the *zmdreb2a* seeds, with decreased expression of *RAFFINOSE SYNTHASE* (*ZmRAFS*) and less raffinose in their embryo, exhibit decreased seed aging tolerance, than the NS controls. Overexpression of *ZmDREB2A* in maize protoplasts increased the expression of *ZmGH3.2*, *ZmRAFS* genes and that of a *Rennila* LUCIFERASE reporter (*Rluc*) gene, which was controlled by either the *ZmGH3.2*- or *ZmRAFS*-promoter. Electrophoretic mobility shift assays and chromatin immunoprecipitation assay quantitative polymerase chain reaction showed that ZmDREB2A directly binds to the DRE motif of the promoters of both *ZmGH3.2* and *ZmRAFS*. Exogenous supplementation of IAA to the unaged, germinating NS seeds increased subsequent seedling growth making them similar to the *zmdreb2a* seedlings from unaged seeds. These findings provide evidence that *ZmDREB2A* regulates the longevity of maize seed by stimulating the production of raffinose while simultaneously acting to limit auxin-mediated cell expansion.

Keywords: maize (*Zea Mays*), DREB2A, seedling growth, seed aging tolerance, IAA, raffinose.

INTRODUCTION

The response of plants to abiotic stresses is complex (Zhu, 2016). The inevitability of encountering such stresses in the field, and the consequent reduction in crop yield incurred, has prompted efforts to understand reactions to these stresses while minimizing their influence on the harvestable entity (Sehgal *et al.*, 2019). Thus, identification of regulatory hubs controlling the effects of the stress(es) on crop yield and an understanding of the multifarious components impinging on, radiating from, the hub (Cramer *et al.*, 2011) have been prioritized in efforts to alter these processes to maximize the production of food (Wang *et al.*, 2018). One such regulatory hub is embodied in the DEHYDRATION-RESPONSIVE ELEMENT BINDING PROTEIN (DREB) family of transcription factors (TF), which plays a central role in vegetative abiotic stress responses (Yamaguchi-Shinozaki and Shinozaki, 1994; Liu *et al.*, 1998; Nakashima *et al.*, 2000; Qin *et al.*, 2007). The Arabidopsis DREB proteins were divided into six subgroups designated A1–A6. The subgroup A1 (DREB1s) contains cold- and drought-responsive

© 2020 Society for Experimental Biology and John Wiley & Sons Ltd

TFs, such as DREB1A, while the subgroup A2 (DREB2s) contains drought-, salt- and heat-responsive TFs, for example DREB2A (Nakano *et al.*, 2006). Alternative splicing of maize *DREB2A* (*ZmDREB2A*) produces two *ZmDREB2A* transcripts, the longer inactive transcript is expressed under normal conditions while the shorter active transcript is expressed under stress conditions (Qin *et al.*, 2007). DREB TFs bind to the C-repeat (GCCGAC) or the DRE (ACCGAC) core motif in the promoter of its target genes and activates gene expression in response to abiotic stresses (Stockinger *et al.*, 1997; Kasuga *et al.*, 1999; Kasuga *et al.*, 2004). Although, constitutively, overexpression of *DREB1A* or *DREB2A* in Arabidopsis enhanced the plant freezing-, drought-, heat- and high salinity-tolerance; however, the transgenic plants are smaller than the wild-type plants when the plants were grown under optimal conditions (Jaglo-Ottosen *et al.*, 1998; Liu *et al.*, 1998; Gu *et al.*, 2016). Overexpression of *AtDREB1A* (*CBF3*) in Arabidopsis decreased the indole-3-acetic acid (IAA) accumulation in young tissues of the plants (Li *et al.*, 2017a). Overexpression of the *ZmDREB4.1* (a member of DREB A4 subfamily) in tobacco decreased the contents of cytokinin and auxin in leaves and repressed leaf extension and hypocotyl, petiole and stem elongation (Li *et al.*, 2018). Currently, the molecular mechanism by which DREBs regulate IAA accumulation in plant cells remains unknown.

IAA, the major form of natural auxin, is a central hormone regulating plant growth and development. The accumulation of IAA in the plant cell is determined by the amalgam of IAA synthesis, transport and degradation (Feng *et al.*, 2015; Matthes *et al.*, 2019). IAA is synthesized in two steps. The first step uses TAA family AMINOTRANSFERASEs to convert tryptophan to indole-3-pyruvate (Stepanova *et al.*, 2008; Tao *et al.*, 2008). The second step uses the YUCCA (YUC) family of flavin-containing monooxygenases to convert indole-3-pyruvate to IAA (Stepanova *et al.*, 2011; Dai *et al.*, 2013). There are six *TAA* and nine *YUC* genes in maize (Matthes *et al.*, 2019). Auxin transportation from its sites of synthesis to other parts of the plant is essential for plant developmental processes. There are several known families of auxin transporters, PIN-FORMED (PIN), ATP-BINDING CASSETTE FAMILY B (ABCB) and AUXIN1/LIKE-AUX1s (AUX/LAX) (Matthes *et al.*, 2019). There are 11 *PIN* genes, 13 *ABCB* genes and five *AUX/LAX* genes that have been characterized or predicted in maize (Matthes *et al.*, 2019). GRETCHEN HAGEN3s (GH3s) and DIOXYGENASE OF AUXIN OXIDATION (DAOs) are responsible for IAA degradation (Mellor *et al.*, 2016; Porco *et al.*, 2016; Zhang *et al.*, 2016). DAO is more important than GH3 in IAA degradation when the auxin level is low, while GH3 plays a major role when the auxin level is high (Mellor *et al.*, 2016). There are 13 members of *GH3s* and two of *DAOs* in maize (Feng *et al.*, 2015; Porco *et al.*, 2016). Owing to the functional conservation and redundancy of the relevant genes in maize IAA biosynthesis, transport and degradation pathways, the function and expression regulation of each individual gene remains largely unknown.

Raffinose family oligosaccharides play important roles in seed vigor (Koster and Leopold, 1988; Bernal-Lugo and Leopold, 1992; Li *et al.*, 2017b). GALACTINOL SYNTHASE (GOLS; inositol 3-alpha-galactosyltransferase; EC2.4.1.123; Saravitz *et al.*, 1987) and RAFFINOSE SYNTHASE (RAFS; galactinol-sucrose galactosyltransferase; EC2.4.14.82; Peterbauer *et al.*, 2002) are two committed enzymes for raffinose family oligosaccharide biosynthesis. Previous investigation into the regulation of raffinose biosynthesis has mainly focused on the transcriptional regulation of *GOLS*. Both Arabidopsis *AtGOLS1-* and *-2* are induced by drought and salt stress while *AtGOLS3* is induced by cold stress. Overexpression of *AtGOLS2* increased the galactinol and raffinose content and enhanced plant drought stress tolerance in Arabidopsis (Taji *et al.*, 2002), and increased the grain yield in rice under dry field conditions (Selvaraj *et al.*, 2017). ZmVP1 interacts with ZmABI5 and regulates *ZmGOLS2* expression in maize protoplast cells (Zhang *et al.*, 2019). ZmDREB2A directly upregulates the expression of *ZmGOLS2* in maize protoplast cells and overexpression of either *ZmDREB2A* or *ZmGOLS2* in Arabidopsis enhanced vegetative abiotic stress tolerance (Gu *et al.*, 2016). Unlike *GOLS*, the regulation of *RAFS* remains unclear except for a single report whereby overexpression of the *Brassica napus HEAT SHOCK TRANSCRIPTION FACTOR A4A* (*BnHSFA4a*) in Arabidopsis upregulates the expression of Arabidopsis *RAFFINOSE SYNTHASE2* gene (Lang *et al.*, 2017).

The hyperaccumulation of IAA in the *zmdreb2a* zygotic embryo permitted maize seedlings to grow faster following the completion of germination than the null segregant (NS) control. This was despite lower amounts of raffinose in the mutant, a sugar suggested as a source of energy during germination and for seedling establishment following the completion of germination (Downie and Bewley, 2000; Gangl and Tenhaken, 2016). However, the artificial aging tolerance of *zmdreb2a* seeds decreased compared with that of their NS control, a phenomenon linked to less than optimal raffinose amounts in the embryos (Li *et al.*, 2017b). We found, that ZmDREB2A directly upregulated *ZmGH3.2*, which, in the *zmdreb2a* mutant embryo, resulted in the greater IAA concentration. Simultaneously, the reduced raffinose content in the *zmdreb2a* embryo is attributable to the lack of direct DREB2A transcriptional stimulation of *ZmRAFS*. These results suggest that the TF ZmDREB2A regulates the balance between IAA-stimulated seedling growth and raffinose-mediated seed aging tolerance.

RESULTS

ZmDREB2A suppresses maize seedling growth, while stimulating seed aging tolerance

The role of the *ZmDREB2A* in maize seed germination was examined using two *mutator* (*Mu*)-inserted *zmdreb2a* lines

© 2020 Society for Experimental Biology and John Wiley & Sons Ltd,

(W22 background). The two heterozygous mutant lines were selfed to generate homozygous *zmdreb2a-1* and *zmdreb2a-2* and their respective NS lines, NS-1 and NS-2. Individual plants from the seeds of these crosses were screened by polymerase chain reaction (PCR) to recover individuals that were homozygous for *Mu* insertion or the corresponding NS (Figure 1a and Figure S1a). PCR using different primer pairs determined that *Mu* inserted in the promoter region of *ZmDREB2A* gene for both *zmdreb2a-1* and *zmdreb2a-2* (Figure 1b and Figure S1b). Sequencing the PCR amplicons (using a *Mu*-specific primer [MU25] and gene-specific primers [F1a, R1a]) revealed a stereotypical 9-bp duplication juxtaposing the *Mu* element and the exact location of the insertion in both mutant lines, which differed by only 22 nt (Figure 1a and Figure S1a). Despite the promoter location of the insertions, transcription of *ZmDREB2A* was inhibited in the mutants as determined by reverse transcription (RT)-PCR using primers F2a and R2a (Figure 1c and Figure S1c). Less ZmDREB2A protein accumulation was detected in the nucleus of the *zmdreb1* embryos detached from 35 days after pollination (DAP) seeds, as compared with its NS controls, using Western blot hybridization (Figure 1d and Figure S1d). Despite the apparent decreased *ZmDREB2A* expression in both mutant lines, the moisture content of the seed components and the 1000-seed weights between the mutants and their respective NSs, were statistically indistinguishable (Figure S2a–c). Plant stature and leaf appearance were also statistically identical when the appropriate NS and *zmdreb2a* were compared (Figure S2d).

The cumulative germination percentage of NS and *zmdreb2a* seeds was tested with or without accelerated aging (AG) treatment (Figure 1e and Figure S1e). There was no difference of germination percentage between the *zmdreb2a-1* mutant and its NS-1 when the seeds were not treated with AG (Figure 1f). However, after AG treatment for 6 days (AG6), the germination percentage of *zmdreb2a-1* seeds was significantly less than that of NS-1 control at

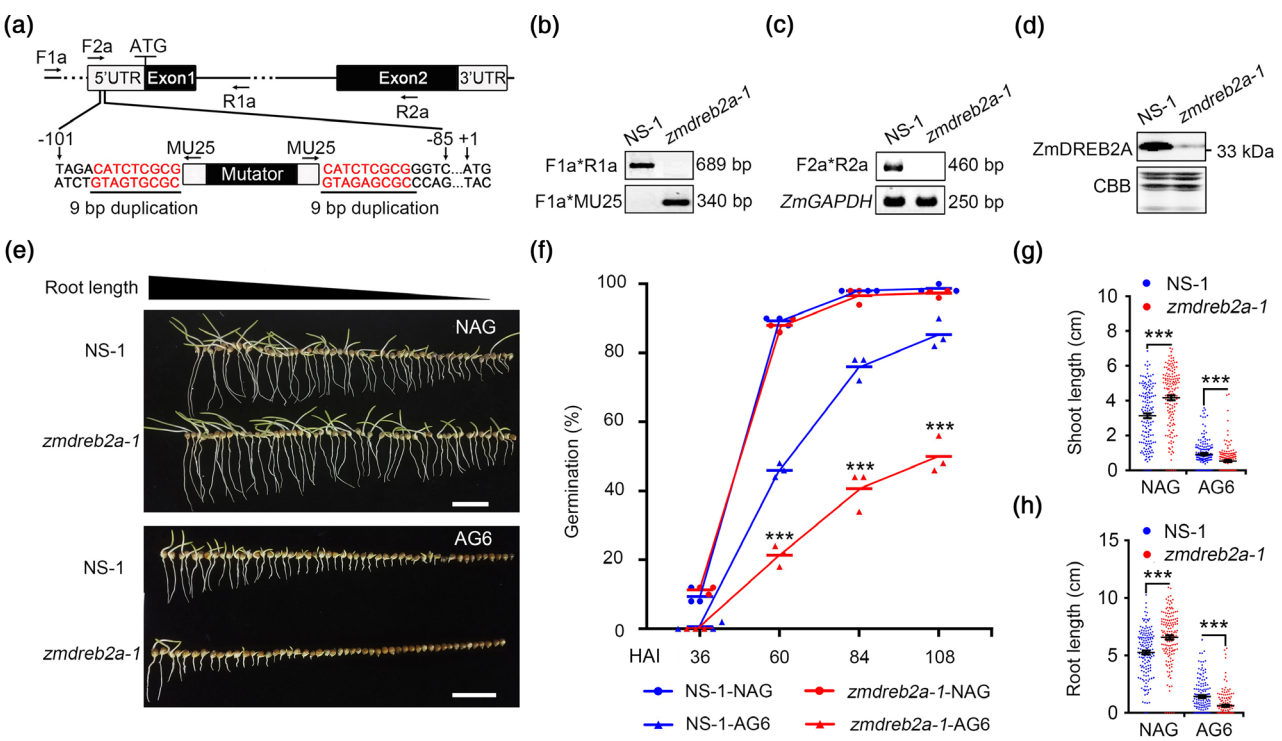

Figure 1. ZmDREB2A suppresses maize seedling growth, while stimulating seed aging tolerance.
(a) Structure of the *ZmDREB2A* gene and mutator insertion of the *zmdreb2a-1* mutant. Exons are shown as black boxes and introns as lines. 5′UTR and 3′UTR are shown as white boxes. Mutator insertion site and primer sites are indicated. (b) Polymerase chain reaction characterization of the genotype of the null segregant (NS) and *zmdreb2a-1* mutant plants. (c) Reverse transcription–polymerase chain reaction analysis of *ZmDREB2A* transcript abundance in NS and *zmdreb2a-1* plants. (d) Western blot analysis of ZmDREB2A protein accumulation (top panel) in nucleus of the seed embryo of NS-1 and *zmdreb2a-1* mutants. Coomassie® brilliant blue staining (CBB) of the same amount of nuclear protein as used in Western blot analysis was used as the loading control. (e) Photographs of one replicate of NS and *zmdreb2a-1* seeds/seedlings after imbibition for 120 h without accelerated aging (AG) or following AG for 6 days (AG6). White scale bar represents 5 cm. NAG, no AG treatment. (f) Comparison of seed germination between NS-1 and *zmdreb2a-1* seeds that were either left untreated or AG treated. Seeds were imbibed at 28°C in the dark and the completion of germination was monitored every 24 h, by briefly observing them under low light, from 36 HAI to 108 HAI. HAI, hours after imbibition. Scatter plots with mean are depicted. Each dot or triangle represents one biological replicate (50 seeds) and there are three biological replicates. Values are means ± SE ($n = 3$). ***$P < 0.001$ (Student's *t*-test). (g–h) Comparison of shoot length (g) and root length (h) of seedlings generated in (e). Scatter plots with mean are depicted. Each dot represents one biological replicate and there are 150 biological replicates. Values are means ± SE ($n = 150$). ***$P < 0.001$ (Student's *t*-test).

© 2020 Society for Experimental Biology and John Wiley & Sons Ltd,

all time points except 36 HAI (Figure 1f). Both shoot and root lengths of *zmdreb2a-1* seedlings were significantly longer than that of the NS-1 control for no AG (NAG) treatment (Figure 1g,h). In contrast, the shoot and root lengths of *zmdreb2a-1* seedlings were significantly shorter than that of the NS-1 control after AG6 treatment (Figure 1g,h). A similar phenotype was observed in *zmdreb2a-2* mutants where root lengths for non-aged mutants were greater than that of the NS-2 while, following 6 days AG, both root and shoot lengths were less than the NS-2 (Figure S1g,h).

Supplementation of IAA to germinating seeds eliminated the shoot/root length difference of NS relative to the *zmdreb2a* mutant

To investigate the biochemical and molecular mechanisms by which *zmdreb2a* seedlings grew faster than that of their NS controls, the hormones in the embryo between *zmdreb2a* and its NS controls were compared. The IAA content in *zmdreb2a-1* embryos was almost double, and was significantly greater than those of the NS-1 controls were (Figure 2a). The IAA content in *zmdreb2a-2* embryos was also significantly greater than that of the NS-2 control (Figure S3a). To determine whether ZmDREB2A inhibits maize seedling growth by inhibition of bioactive IAA accumulation we tested if supplementation of exogenous IAA to germinating seeds would stimulate subsequent seedling growth to the point where differences would be mitigated if not eliminated (Figure 2b,c). The shoot and root length of *zmdreb2a*-1 seedlings was significantly greater than that of NS-1 controls without IAA supplementation (Figure 2b,c and Figure S4). The shoot length of the NS-1 increased when the germinating seeds were supplemented with 4 μM IAA (Figure 2b) to the point where there was no longer a difference in shoot length between *zmdreb2a-1* and NS-1 (Figure 2b). However, this was due partly to an increase in NS-1 shoot length and partly to a decrease in *zmdreb2a-1* shoot length as exogenous IAA increased (Figure 2b). The root length of both NS and *zmdreb2a*-1 seedlings was significantly increased when the germinating seeds were supplemented with 2 μM IAA, but the relative increase was greatest for the NS-1 seedlings (Figure 2c). When the IAA concentration was increased to 4 μM, the root length of *zmdreb2a-1* seedlings decreased and there was no root length difference between NS and *zmdreb2a-1* mutant seedlings (Figure 2c). Because of the difference of IAA content in seed embryos of the NS-1, *zmdreb2a-1*, NS-2 and *zmdreb2a-2* lines (Figure 2a and Figure S3a), the response of germinating seeds to the exogenous IAA was different. The shoot and root length of *zmdreb2a*-2 seedlings was significantly greater than that of the NS-2 control when the

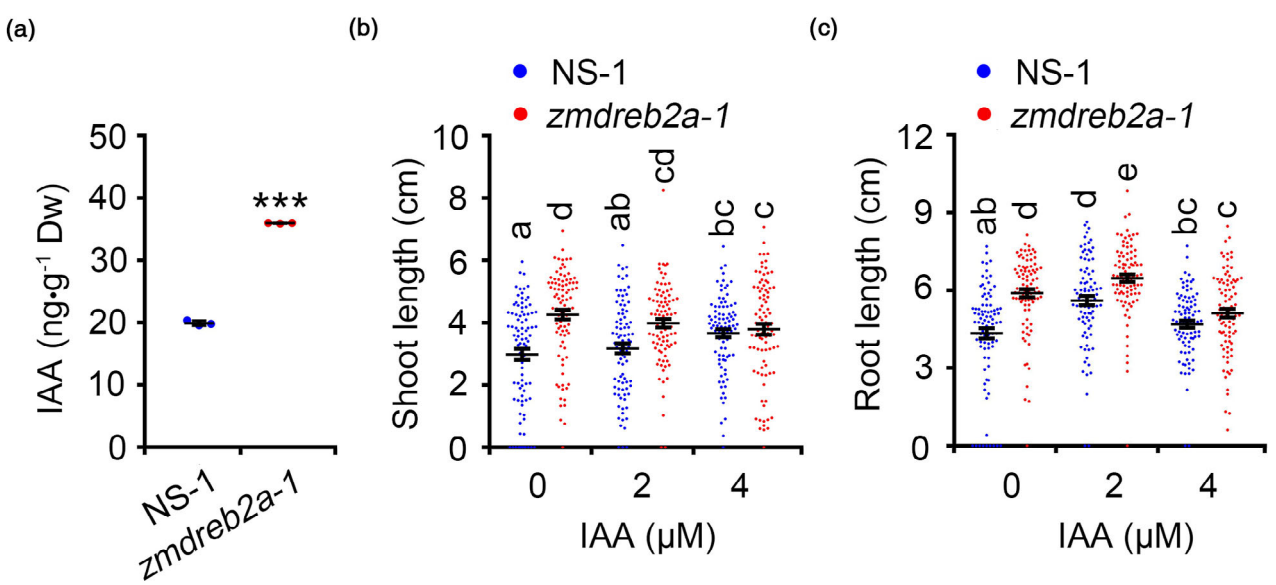

Figure 2. Supplementation of indole-3-acetic acid (IAA) to germinating seeds eliminated the shoot/root length phenotype of NS relative to the *zmdreb2a* mutant.
(a) Comparison of IAA contents from embryos between NS and *zmdreb2a-1*. Embryos were separated from mature seeds. Scatter plots with mean are depicted. Each dot represents one biological replicate (50 embryos) and there are three biological replicates. Values are means ± SD ($n = 3$). ***$P < 0.001$ (Student's *t*-test). Dw, dry weight; NS, null segregant.
(b) Comparison of shoot length of seedlings between NS-1 and *zmdreb2a-1* mutants treated with different IAA concentrations after imbibition for 120 h. NS and *zmdreb2a-1* seeds were germinated in 0, 2 or 4 μM IAA. Scatter plots with mean are depicted. Each dot represents one biological replicate (one seed) and there are 90 biological replicates. Values are means ± SE ($n = 90$). Different lowercase letters denote significant differences (Duncan test).
(c) Comparison of root length of seedlings between NS-1 and *zmdreb2a-1* mutants treated with different IAA concentrations after imbibition for 120 h. NS and *zmdreb2a-1* seeds were germinated in 0, 2 or 4 μM IAA. Scatter plots with mean are depicted. Each dot represents one biological replicate (one seed) and there are 90 biological replicates. Values are means ± SE ($n = 90$). Different lowercase letters denote significant differences (Duncan test).

© 2020 Society for Experimental Biology and John Wiley & Sons Ltd,

germinating seeds were on water (Figure S5). There was no difference of the shoot and root length of the seedlings between *zmdreb2a-2* and its NS-2 controls when the germinating seeds were supplemented with 0.5 or 1 μM IAA (Figure S5).

ZmDREB2A upregulates the expression of IAA (auxin) deactivating enzyme gene *ZmGH3.2*

To investigate why IAA increased in *zmdreb2a* mutant embryos, *ZmDREB2A* or *GFP* expression vectors were constructed and transformed into the maize mesophyll protoplasts for comparison of the gene expression changes induced by ZmDREB2A. The *ZmDREB2A* mRNA expression and ZmDREB2A protein accumulation in maize protoplasts transformed with the *ZmDREB2A* expression vector were significantly greater than that of *GFP*-expressing cells (Figure 3a,b). The transcriptome of the *ZmDREB2A* overexpressing protoplasts was compared with that of the *GFP* overexpressing cells and all statistically significantly differentially expressed genes listed (Table S1). As IAA was increased in *zmdreb2a* mutant embryos, we directed our investigation to the relevant genes whose encoded proteins are involved in IAA synthesis, transport and degradation for analysis of RNA-sequencing (RNA-Seq) data. There was no difference of expression level of genes related to IAA biosynthesis or transport between *GFP* and

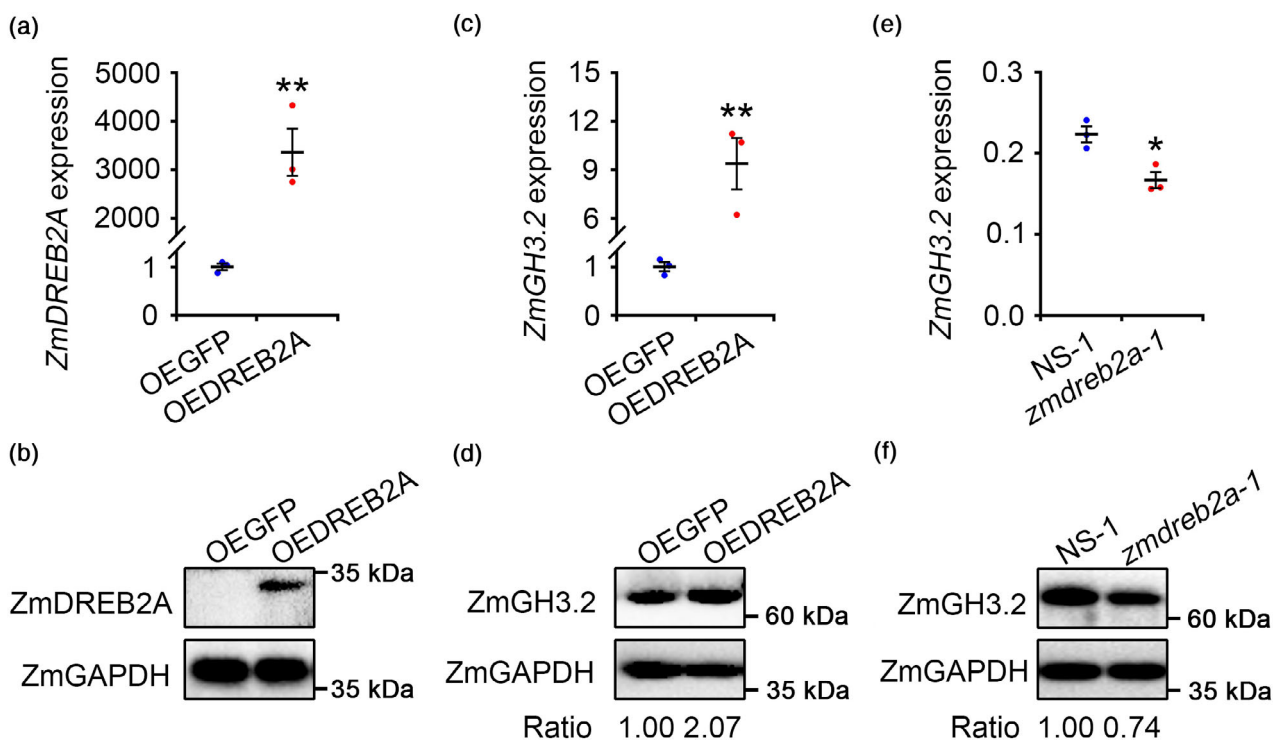

Figure 3. ZmDREB2A stimulates indole-3-acetic acid (IAA) degradation by directly upregulating *ZmGH3.2* expression.
(a) Comparison of *ZmDREB2A* mRNA accumulation in maize mesophyll protoplasts that were transformed with either *GFP* or the *ZmDREB2A* expression vector by real time reverse transcription–polymerase chain reaction analysis. mRNA was extracted from protoplasts 17 h after transformation. Expression of *ZmDREB2A* mRNA was normalized to the expression of maize *GAPDH* and is presented relative to the *GFP* expressing control cells. Scatter plots with mean are depicted. Each dot represents one biological replicate and there are three biological replicates. Values are means ± SE ($n = 3$). $^{**}P < 0.01$ (Student's *t*-test). (b) Western blot analysis of ZmDREB2A accumulation in maize mesophyll protoplasts that were transformed with either *GFP* or the *ZmDREB2A* expression vector. Proteins were extracted from protoplasts 17 h after transformation and then were analyzed for ZmDREB2A expression by Western blot using ZmDREB2A antibody. GAPDH antibody was used as an internal control. (c) Comparison of *ZmGH3.2* mRNA expression in maize mesophyll protoplasts that were transformed with either *GFP* or the *ZmDREB2A* expression vector by real time reverse transcription–polymerase chain reaction analysis. mRNA were extracted from protoplasts 17 h after transformation. Expression of *ZmGH3.2* mRNA was normalized to the expression of maize *GAPDH* and is presented relative to the GFP expressing control cells. Scatter plots with mean are depicted. Each dot represents one biological replicate and there are three biological replicates. Values are means ± SE ($n = 3$). $^{**}P < 0.01$ (Student's *t*-test). (d) Western blot analysis of ZmGH3.2 accumulation in maize mesophyll protoplasts that were transformed with either *GFP* or the *ZmDREB2A* expression vector. GAPDH antibody was used as an internal control (the Western blots were performed at different date using the same batch of proteins as described in b). (e) Comparison of *ZmGH3.2* mRNA accumulation in embryos between null segregant (NS) and the *zmdreb2a-1* mutant as determined by real time reverse transcription–polymerase chain reaction analysis. RNA was extracted from DAP35 embryos from the *zmdreb2a-1* mutant or NS-1. DAP, days after pollination. Expression of *ZmGH3.2* mRNA was normalized to the expression of maize *GAPDH* and is presented relative to the NS control embryos. Scatter plots with mean are depicted. Each dot represents one biological replicate (five embryos) and there are three biological replicates. Values are means ± SE ($n = 3$). $^{*}P < 0.05$ (Student's *t*-test). (f) Western blot analysis of ZmGH3.2 protein accumulation (top panel) in NS and *zmdreb2a-1* mutants. Bottom panel is a Western blot analysis of GAPDH protein from the same extracts, demonstrating equal protein loading. Proteins were extracted from DAP35 embryos of the *zmdreb2a-1* mutant or NS.

© 2020 Society for Experimental Biology and John Wiley & Sons Ltd,

ZmDREB2A overexpressing cells (Table S2). The expression of *ZmGH3.2* (*GRETCHEN HAGEN 3.2*) and *ZmDAO1* (*DIOXYGENASE FOR AUXIN OXIDATION 1*), which are related to IAA degradation, was significantly upregulated in *ZmDREB2A* overexpressing protoplasts relative to the *GFP* expressing cells (Table S2).

The upregulation of *ZmGH3.2* gene expression by ZmDREB2A in maize protoplasts was further confirmed by real time RT-PCR (Figure 3c). In addition to the upregulation of *ZmGH3.2* mRNA, ZmGH3.2 protein accumulation was also increased in *ZmDREB2A* overexpressing maize protoplast cells compared with that of the *GFP* expressing cells as determined by Western blot analysis (Figure 3d). Both *ZmGH3.2* mRNA (Figure 3e and Figure S3b) and its protein accumulation (Figure 3f and Figure S3c) were decreased in *zmdreb2a* mutant embryos compared with that of the NS control.

The *ZmGH3.2* 5′-flanking region was identified by searching the genomic database of the maize inbred line B73 (http://blast.maizegdb.org/home.php) using *ZmGH3.2* gene ID number (GRMZM2G378106). The 277 bp of the *ZmGH3.2* 5′ regulatory region (−277 to −1 relative to the start codon AUG) was obtained by PCR and cloned into the pGL3-Basic vector (Figure 4a). There was one DRE in the 5′ regulatory region of *ZmGH3.2* (Figure 4a) as predicted using online databases, PlantCARE (http://bioinformatics.psb.ugent.be/webtools/plantcare/html/), PLACE (http://www.dna.affrc.go.jp/PLACE/) (Higo *et al.*, 1999) and Neural Network Promoter Prediction (http://promotor.biosino.org/). To investigate whether ZmDREB2A regulates *ZmGH3.2* expression through direct binding to the DRE motif in its promoter, the dual luciferase expression vector was used as previously described (Gu *et al.*, 2016). In this instance, *Rluc* expression was

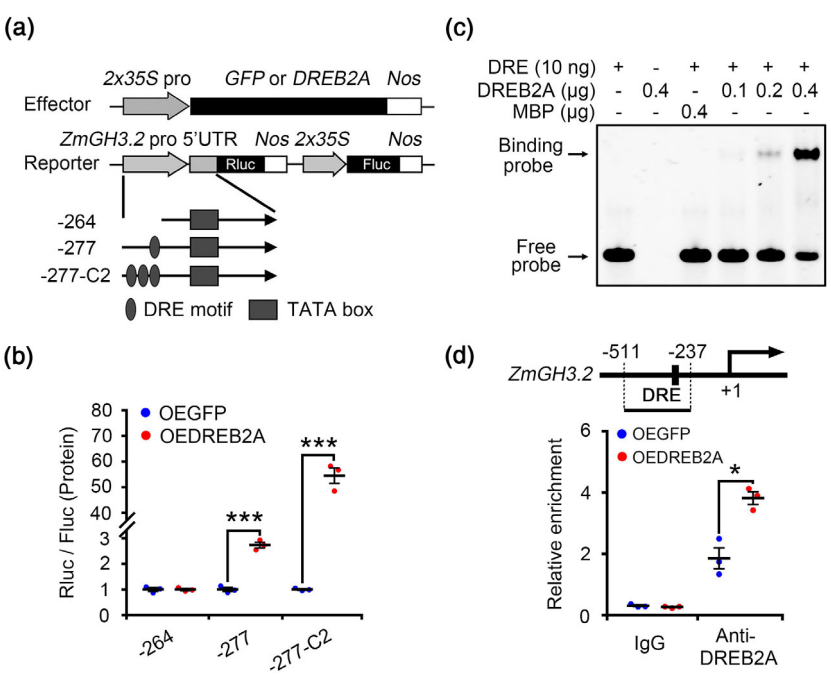

Figure 4. ZmDREB2A binds to the DRE motif of the *ZmGH3.2* promoter and upregulates the expression of *ZmGH3.2*.

(a) Schematic representations of the constructs used for maize protoplast transformation. *GFP* or *ZmDREB2A* expression vector was used as an effector, and the dual luciferase expression vector in which *Rluc* expression was driven by a series of *ZmGH3.2* promoter fragments and *Fluc* expression was driven by the 2× *35S* promoter, were used as reporters. *ZmGH3.2* promoter fragments were without DRE or with one or three copies of DRE. Position of the DREs (ovals) and the TATA box (rectangle) are indicated. Fluc, coding region of firefly luciferase gene; Nos, nopaline synthase terminator; *Rluc*, coding region of *Renilla* luciferase gene; 2× 35S, two copies of the cauliflower mosaic virus 35S promoter.

(b) Relative expression of *Renilla* luciferase in maize protoplasts transformed with the vectors indicated in (a). Scatter plots with mean are depicted. Each dot represents one biological replicate and there are three biological replicates. Values are means ± SE ($n = 3$). ***$P < 0.001$ (Student's *t*-test).

(c) ZmDREB2A binds to the DRE element of the *ZmGH3.2* promoter in vitro. An electrophoretic mobility shift assay was performed by incubation of 10 ng of DRE probe with various amounts of recombinant MBP-DREB2A or 1.6 μg MBP. MBP-DREB2A protein alone, or probes incubated with the MBP tag, served as negative controls.

(d) Chromatin immunoprecipitation quantitative polymerase chain (ChIP qPCR) reactive characterization of the ZmDREB2A binding to the DRE motif in the *ZmGH3.2* promoter. Top panel: schematic diagram of the promoter region of *ZmGH3.2*. Black line represents the promoter region of *ZmGH3.2*, and black box on the line represents the identified DRE motif (ACCGACAG; −270 to −277 bp). Numbers depict the position relative to the start codon ATG (+1 and bent arrow). DNA fragment between the two dotted lines (−511 to −237) indicates the amplified *ZmGH3.2* promoter fragment in ChIP qPCR. Bottom panel, ChIP qPCR characterization of the enrichment of the *ZmGH3.2* promoter fragment. Enrichment of *ZmGH3.2* was normalized to the input (PCR amplification of the genomic DNA without immune precipitation). IgG antibody was used as a negative control. Scatter plots with mean are depicted. Each dot represents one biological replicate and there are three biological replicates. Values are means ± SE ($n = 3$). *$P < 0.05$ (Student's *t*-test).

© 2020 Society for Experimental Biology and John Wiley & Sons Ltd,

controlled by different lengths of the *ZmGH3.2* promoter with one, three (two are introduced copies [−277-C2]), or no copies of the DRE motif. Upon co-transformation into maize protoplasts with either *ZmDREB2A* or *GFP* (negative control) expression vectors, the two luciferase activities were determined (Figure 4a). There was no difference in *Rluc* activity in the cells that were transformed with the dual luciferase vector in which *Rluc* was controlled by the 264-bp *ZmGH3.2* promoter fragment (without DRE) when either *GFP* or *ZmDREB2A* was simultaneously overexpressed in the same cells (Figure 4b). *Rluc* expression controlled by the *ZmGH3.2* promoter containing one or three DRE elements was significantly increased by concurrent *ZmDREB2A* expression when compared with *Rluc* expression when *GFP* (control) was co-expressed (Figure 4b). The ZmDREB2A protein was able to bind to the DRE element of the *ZmGH3.2* promoter *in vitro* as determined by DNA-electrophoretic mobility shift assay (EMSA) (Figure 4c) or *in vivo* as determined by chromatin immunoprecipitation (ChIP) quantitative PCR (Figure 4d). Besides *ZmGH3.2*, another IAA degrading enzyme gene *ZmDAO1* was significantly upregulated by *ZmDREB2A* overexpression in maize protoplasts (Figure S6).

To investigate whether *ZmDREB2A* is upregulated by seed maturation desiccation, a developmentally imposed stress, the mRNA accumulation of *ZmDREB2A* in zygotic embryos was determined at 21, 28 and 35 DAP during seed development. The *ZmDREB2A* mRNA transcripts increased dramatically in zygotic embryos at 28 DAP compared with that of 21 DAP, and increased still further at 35 DAP (Figure S7a). The mRNA abundance of *ZmGH3.2* and *ZmRAFS* also increased in zygotic embryos at 28 DAP, compared with that of 21 DAP, and it was increased further at 35 DAP (Figure S7b,c).

AG6 treatment significantly upregulated the expression of *ZmDREB2A* and *ZmGH3.2*, and tended to do the same for *ZmRAFS* relative to unaged, unimbibed embryos (NAG, 0 h after imbibition [HAI]; Figure S7d–f). At 24 and 48 HAI, expression of *ZmDREB2A*, *ZmGH3.2* and *ZmRAFS* was significantly stimulated in AG6 seed embryos compared with that of NAG seeds (Figure S7d–f). Compared with 0 HAI in NAG seeds, *ZmDREB2A* expression remains unchanged during seed imbibition from 24 to 72 HAI. In AG seeds, *ZmDREB2A* expression did not change from 0 to 24 HAI, but declined at 48 and 72 HAI (Figure S7d). *ZmGH3.2* mRNA amounts in NAG seed embryos rose significantly following imbibition declining only at 72 HAI, when it was still above that at 0 HAI (Figure S7e). There was no change for *ZmRAFS* expression during seed imbibition in NAG seeds (Figure S7f), while in AG seeds, *ZmRAFS* mRNA accumulation was not changed at 24 HAI, but increased at 48 HAI and then decreased at 72 HAI (Figure S7f).

ZmDREB2A enhances raffinose biosynthesis through upregulation of *ZmRAFS* expression

As our previous findings has demonstrated that raffinose is critical for maize seed vigor (Li *et al.*, 2017b), we focused on genes whose encoded proteins are relevant to the raffinose metabolism pathway for analysis of RNA-Seq data. RNA-Seq data showed that RAFS (GRMZM2G150906, inappropriately labeled "STACHYOSE SYNTHASE" in the maize database), the gene encoding the key enzyme responsible for raffinose biosynthesis, was upregulated in *ZmDREB2A* overexpressing maize protoplast cells compared with that of *GFP*-expressing cells (Table S1). The upregulation of *ZmRAFS* by *ZmDREB2A* overexpression in maize protoplasts was also confirmed by real time RT-PCR (Figure 5a). Furthermore, expression of *ZmDREB2A* in maize protoplast cells significantly increased the protein accumulation of endogenous ZmRAFS compared with cells overexpressing *GFP* (Figure 5b). The *ZmRAFS* mRNA abundance and its protein accumulation were significantly decreased in the 35 DAP embryos of *zmdreb2a-1* plants compared with that of the NS controls (Figure 5c,d). There was no difference of sucrose or galactinol amounts in 35 DAP embryos between *zmdreb2a-1* and its NS-1 controls (Figure 5e,f). The raffinose content in *zmdreb2a-1* embryo was significantly decreased compared with that of NS-1 controls (Figure 5g). The mRNA and protein accumulation of *ZmRAFS* both trended downward in the *zmdreb2a-2* embryo compared with that of the NS controls (Figure S8a,b). There was no difference of sucrose or galactinol amounts in 35 DAP embryos between *zmdreb2a-2* and its NS-2 controls (Figure S8c,d). The raffinose content in the *zmdreb2a-2* embryo also tended to decrease compared with that of the NS-2 control (Figure S8e). The *ZmRAFS* 5′-flanking region was identified by searching the genomic database of the maize inbred line B73 (http://blast.maizegdb.org/home.php) using *ZmRAFS* gene ID number (GRMZM2G150906) as the query. The 208 bp of the *ZmRAFS* 5′ regulatory region (−208 to −1 relative to the start codon AUG) was obtained by PCR and cloned into the pGL3-Basic vector. The sequence of the *ZmRAFS* promoter was analyzed for all putative *cis*-acting elements using the databases as mentioned above. A single predicted DRE motif in the 5′ regulatory region of *ZmRAFS* was identified (Figure 6a). To investigate whether ZmDREB2A regulates the expression of *ZmRAFS* through binding to this DRE motif in the *ZmRAFS* promoter, the dual luciferase expression vectors, in which *Rluc* expression was controlled by different lengths of *ZmRAFS* promoter fragments with one or three (two of which are additional, introduced copies [−208-C2]) copies of the DRE motif or without the DRE motif, was co-transformed into maize protoplasts with either *ZmDREB2A* or *GFP* expression vector and the two luciferase activities determined

© 2020 Society for Experimental Biology and John Wiley & Sons Ltd,

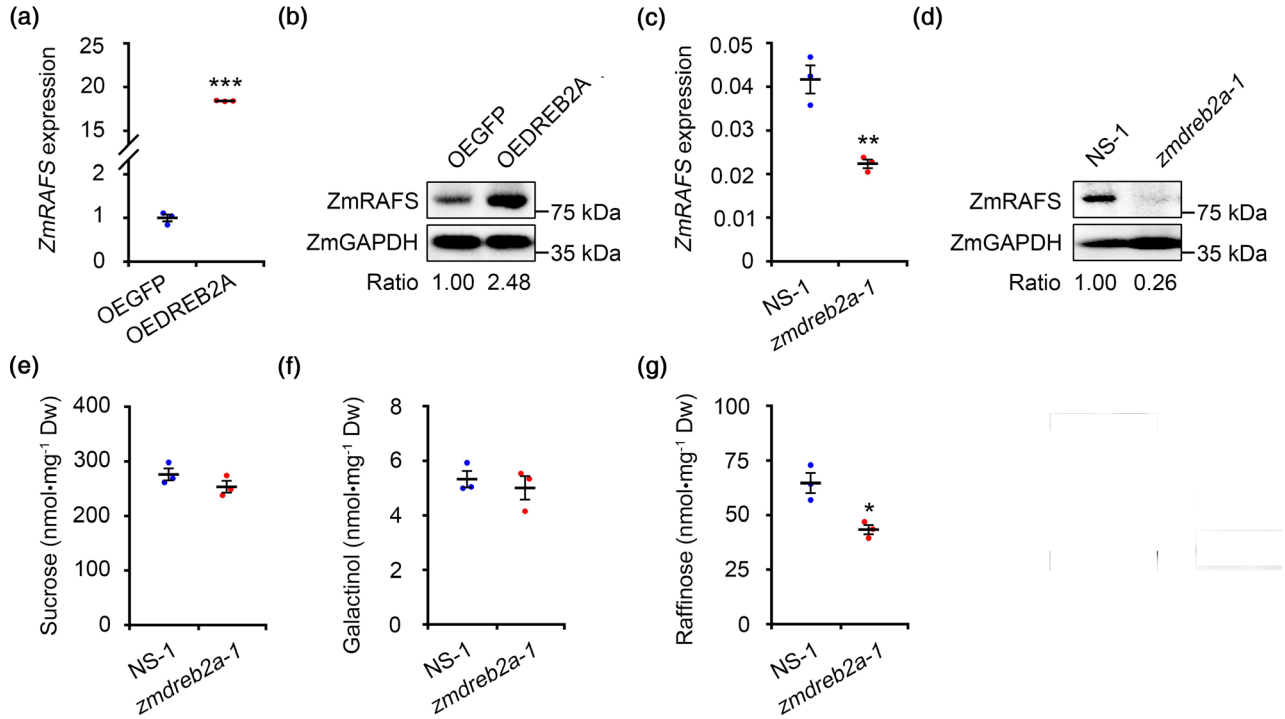

Figure 5. ZmDREB2A enhances raffinose accumulation through upregulation of *ZmRAFS* expression.
(a) Comparison of *ZmRAFS* mRNA expression in maize mesophyll protoplasts that were transformed with either *GFP* or the *ZmDREB2A* expression vector by real time reverse transcription–polymerase chain reaction analysis. mRNA were extracted from protoplasts 17 h after transformation. Expression of *ZmRAFS* mRNA was normalized to the expression of maize *GAPDH* and is presented relative to the *GFP* expressing control cells. Scatter plots with mean are depicted. Each dot represents one biological replicate and there are three biological replicates. Values are means ± SE ($n = 3$). ***$P < 0.001$ (Student's *t*-test). (b) Western blot analysis of ZmRAFS accumulation in maize mesophyll protoplasts that were transformed with either *GFP* or *ZmDREB2A* expression vector. Same batch of proteins as described in Figure 3(b) were used to analyze for ZmRAFS expression by Western blot using ZmRAFS antibody. ZmGAPDH blot was the same as the GAPDH blot in Figure 3(b). NS, null segregant. (c) Comparison of *ZmRAFS* mRNA accumulation in seed embryos between NS-1 and *zmdreb2a-1* mutant as determined by real time reverse transcription–polymerase chain reaction. RNA was extracted from DAP35 seed embryos of *zmdreb2a-1* mutant or NS. *ZmRAFS* expression was normalized to the *ZmGAPDH* expression. Scatter plots with mean are depicted. Each dot represents one biological replicate (five embryos) and there are three biological replicates. Values are means ± SE ($n = 3$). **$P < 0.01$ (Student's *t*-test). (d) Comparison of ZmRAFS protein accumulation (top panel) between NS-1 and *zmdreb2a-1* mutants as determined by Western blot analysis. Bottom panel is Western blot analysis of ZmGAPDH protein from the same extracts, demonstrating equal protein loading. Proteins were extracted from seed embryos, 35 days after pollination, of *zmdreb2a-1* mutant or NS. (e–g) Comparison of (e) sucrose, (f) galactinol or (g) raffinose contents from embryos between the NS-1 and *zmdreb2a-1* mutant. Embryos were separated from mature seeds. Scatter plots with mean are depicted. Each dot represents one biological replicate (15 embryos) and there are three biological replicates. Values are means ± SE ($n = 3$). *$P < 0.05$ (Student's *t*-test).

(Figure 6a). There was no difference in Rluc activity in the cells transformed with the dual luciferase vector in which *Rluc* was controlled by the 196 bp *ZmRAFS* promoter fragment (without DRE) when either *GFP* or *ZmDREB2A* was simultaneously overexpressed in the same cells (Figure 6b). *Rluc* expression controlled by the *ZmRAFS* promoter containing one (native) or three DRE elements was significantly increased by concurrent *ZmDREB2A* expression when compared with *Rluc* expression when *GFP* (control) was co-expressed (Figure 6b). The ZmDREB2A protein was able to bind to the DRE element of the *ZmRAFS* promoter *in vitro* as determined by DNA-EMSA (Figure 6c) or *in vivo* as determined by ChIP quantitative PCR (Figure 6d).

In conclusion, ZmDREB2A upregulates the expression of both *ZmGH3.2* and *ZmRAFS*, simultaneously decreasing IAA amounts while increasing raffinose titer in zygotic embryos during the late stages of seed development, which in turn enhances seed aging tolerance and inhibits maize seedling growth (Figure 7).

DISCUSSION

DREB2A co-ordinates plant growth and abiotic stress tolerance through regulation of the accumulation of IAA and raffinose

The function and expression regulation of DREB2A in response to vegetative abiotic stress has been extensively investigated. *DREB2A* is induced by abiotic stress and overexpression of *DREB2A* enhances vegetative abiotic stress tolerance while reducing plant growth (Liu *et al.*, 1998; Sakuma *et al.*, 2006a; Sakuma *et al.*, 2006b; Qin *et al.*, 2007; Gu *et al.*, 2016). Up to the present, the molecular mechanism of how DREB2A balances the vegetative growth and the plant abiotic stress tolerance remains unknown. Our findings that

© 2020 Society for Experimental Biology and John Wiley & Sons Ltd,

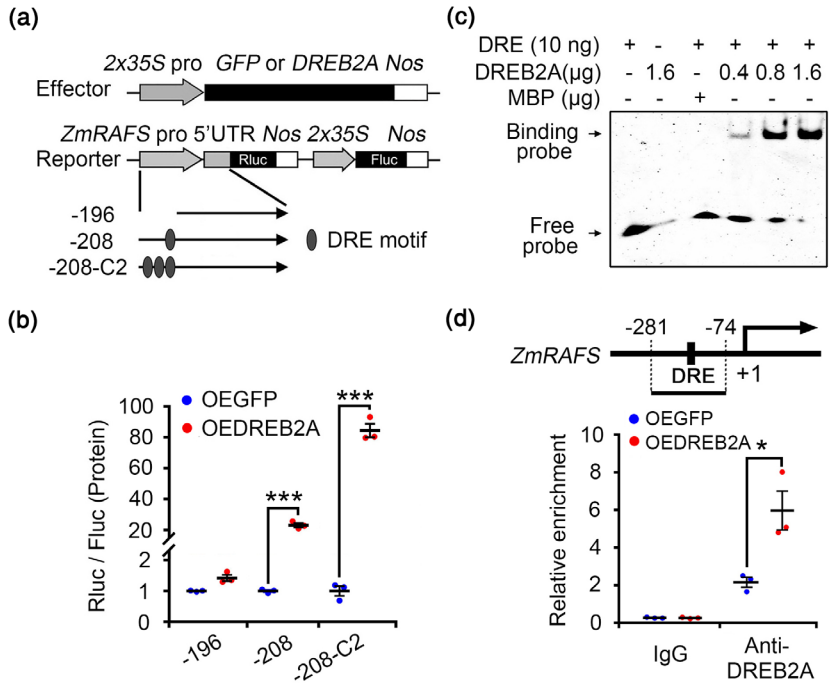

Figure 6. ZmDREB2A binds to the DRE motif of the *ZmRAFS* promoter and upregulates the expression of *ZmRAFS*.
(a) Schematic representations of the constructs used for maize protoplast transformation. GFP or ZmDREB2A expression vector, and the dual luciferase expression vector are the same as described in Figure 4(a) except that *ZmGH3.2* promoter fragments were replaced by the *ZmRAFS* promoter fragments −196, −208 and −208C2.
(b) Relative expression of *Renilla* luciferase in maize protoplasts transformed with the vectors indicated in (a). Scatter plots with mean are depicted. Each dot represents one biological replicate and there are three biological replicates. Values are means ± SE ($n = 3$). ***$P < 0.001$ (Student's *t*-test).
(c) ZmDREB2A binds to the DRE element of *ZmRAFS* promoter in vitro. Legend is the same as described in Figure 4(c).
(d) Chromatin immunoprecipitation quantitative polymerase chain (ChIP qPCR) characterization of the ZmDREB1A binding to the DRE motif in the *ZmRAFS* promoter. Top panel: schematic diagram of the promoter region of *ZmRAFS*. Black line represents the promoter region of *ZmRAFS* and the black box on the line represents the identified DRE motif (ACCGACCT; −199 to −206 bp). Numbers depict the position relative to the start codon ATG (+1 and bent arrow). DNA fragment between the two dotted lines (−284 to −74) indicates the amplified *ZmRAFS* promoter fragment in ChIP qPCR. Bottom panel: ChIP qPCR characterization of the enrichment of the *ZmRAFS* promoter fragment. Enrichment of *ZmRAFS* was normalized to the input (PCR amplification of the genomic DNA without immune precipitation). IgG antibody was used as a negative control. Scatter plots with mean are depicted. Each dot represents one biological replicate and there are three biological replicates. Values are means ± SE ($n = 3$). *$P < 0.05$ (Student's *t*-test).

ZmDREB2A decreased IAA accumulation through upregulation of the IAA deactivating enzyme gene *ZmGH3.2* revealed the mechanism of why *ZmDREB2A* overexpression in plants inhibited the plant growth under optimal growth conditions (Figures 1 and 2). Additionally, others have reported that overexpression of *OsGH3.8* (the protein sequence is 82.71% similar to ZmGH3.2) in rice leaf cells decreased free IAA concentration (Ding *et al.*, 2008). These data demonstrated that ZmDREB2A decreases IAA concentration through upregulation of IAA amino acid conjugation/degradation. That is not to say that the stimulation of the IAA inactivation is the only means by which ZmDREB2A manipulated auxin-mediated growth. The AUX/IAA proteins interact with the AUXIN RESPONSE FACTORs (ARFs) and inhibit their activity, thus, ARFs are unable to activate their target genes (Leyser, 2018). AtDREB2A directly regulates *IAA5* and *IAA19* expression in Arabidopsis (Shani *et al.*, 2017) and, similarly, our data show that ZmDREB2A upregulates the expression of *ZmIAA5*, *ZmIAA8*, *ZmIAA17*, *ZmIAA25* and *ZmIAA30* in maize protoplasts (Figure S6b–f and Table S2). The upregulation of the transcriptional co-repressor *IAA* genes and the reduction of IAA (auxin) by GH3.2 would synergistically suppress ARF gene expression and decrease the biological effects of auxin (IAA), resulting in growth retardation when the *DREB2A* expression is induced by abiotic stress.

Our previous findings show that *ZmGOLS2* (encoding galactinol synthase, the first enzyme in raffinose biosynthetic pathway) is regulated by ZmDREB2A (Gu *et al.*, 2016). Overexpression of *ZmGOLS2* in Arabidopsis increased the raffinose content in leaves and enhanced the plant abiotic stress tolerance (Gu *et al.*, 2016). ZmDREB2A regulated the expression of *ZmRAFS* (encoding raffinose synthase, the second enzyme in raffinose biosynthetic pathway), increased raffinose accumulation and stimulated the maize seed aging tolerance (Figures 5 and 6). These data demonstrate that the expression level of *ZmDREB2A* acts as a balance between plant growth and abiotic stress tolerance (Figure 7).

© 2020 Society for Experimental Biology and John Wiley & Sons Ltd,

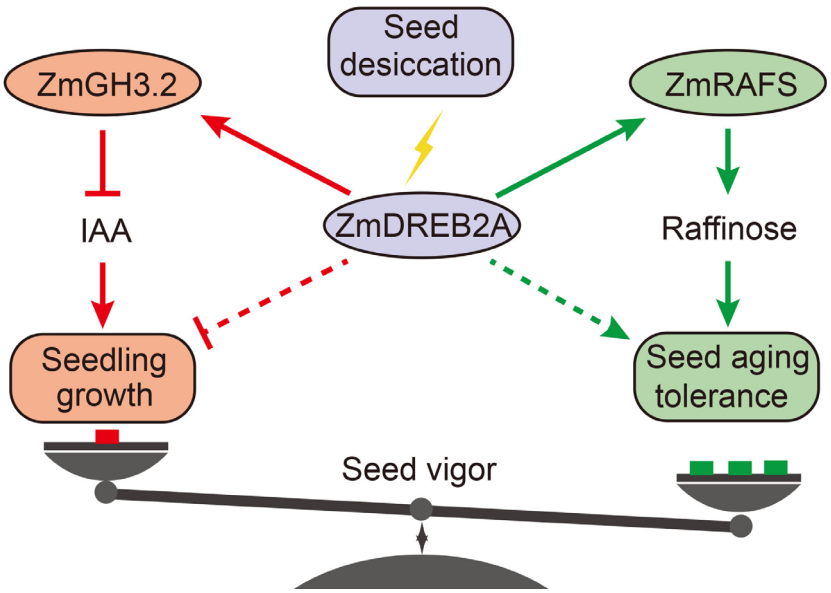

Figure 7. ZmDREB2A regulates the balance between maize seedling growth and seed aging tolerance.
ZmDREB2A upregulates the expression of *ZmGH3.2* and thus decreases the indole-3-acetic acid (IAA) accumulation and inhibits the seedling growth. However, ZmDREB2A would upregulate the *ZmRAFS* expression, increase the raffinose accumulation and increase the seed aging tolerance.

ZmDREB2A plays important roles in seed aging tolerance

Seed maturation desiccation is a natural dehydration process that is programmed into, and encountered by, all orthodox seeds (Angelovici *et al.*, 2010); however, the roles of DREB2A, if any, during the developmentally imposed seed maturation desiccation stress impinging on seed vigor was unclear. The data presented here show that *ZmDREB2A* was induced in zygotic embryos as seed maturation progressed beyond 21 DAP (Figure S7). Concomitantly, the expression of *GH3.2* and *RAFS* followed the same trend (Figure S7). During seed maturation desiccation, the loss of chlorophyll (Clerkx *et al.*, 2003), water replacement (Crowe *et al.*, 1998), generation and stabilization of glasses (Ballesteros and Walters, 2011), alterations of sugar composition (Leprince *et al.*, 2017), production and deployment of intrinsically disordered proteins (Candat *et al.*, 2014), metabolic dampening (Leprince *et al.*, 2000), and nuclear and euchromatin reductions (van Zanten *et al.*, 2011) occur in the seed. Most, if not all of these preparations also reduce the capacity for cell proliferation and elongation (i.e., growth). The simultaneous orchestration of pathways to boost raffinose production, contributing to seed longevity (Li *et al.*, 2017b), while reducing the potential for auxin-mediated growth has illustrated the parallels between vegetative responses to drought stress and seed maturation desiccation, both influenced by ZmDREB2A. During drought stress, the survival over continued growth in vegetative tissues has been largely attributed to abscisic acid (Huot *et al.*, 2014) and the same can be said for seed maturation desiccation where abscisic acid is primarily responsible for many of the events mentioned above that, in the amalgam, prepare the orthodox seed for desiccation and quiescence (Sano *et al.*, 2016). However, in vegetative stress tolerance pathways, another abscisic acid-independent pathway has been identified utilizing DREB2A as a major instigator of the plant's response to stress (Yoshida *et al.*, 2014).

In addition to suppressing maize seedling growth by an inhibition of IAA accumulation, ZmDREB2A enhances seed aging tolerance by stimulation of raffinose accumulation in maize zygotic embryos (Figures 1 and 5, Figures S1 and S8). Because of the direct binding of ZmDREB2A to its *ZmGOLS2* (Gu *et al.*, 2016) and *ZmRAFS* (Figure 6) targets and their subsequent activation, we propose here that ZmDREB2A enhances anabolic raffinose production. However, due to the capacity of ZmDREB2A to downregulate growth simultaneously, it is possible that part of the increase in raffinose might be due to a decline in raffinose catabolism because growth is repressed. One role for raffinose is to provide energy to the germinating seed but this role might also include late stages of seed development. The accumulation of raffinose in *zmdreb2a* mutant seeds is less than that of control NS seeds (Figure 5e and Figure S8c) and the seed aging tolerance of *zmdreb2a* mutant seeds is lower than that of NS seeds (Figure 1 and Figure S1). Our previous work has demonstrated that raffinose and its ratio with sucrose positively regulates maize seed aging tolerance (Li *et al.*, 2017b). These data clearly demonstrate that ZmDREB2A positively controls seed aging tolerance by promoting raffinose accumulation by enhancing its production and, potentially, by reducing its consumption. Transcriptome analysis revealed that 3448 genes were upregulated in seed embryo by AG treatment (Table S3). Among these AG upregulated genes, there were 688 genes that were downregulated in embryos by

© 2020 Society for Experimental Biology and John Wiley & Sons Ltd,

knock down of the *ZmDREB2A* expression in *zmdreb2a-1* mutant seeds compared with that of NS-1 under AG treatment (Table S4). Further analysis showed that 76 genes were upregulated in *ZmDREB2A* overexpressing protoplasts but downregulated in *zmdreb2a-1* mutant AG seed embryos (Figure S9 and Table S5), including *ZmRAFS* and *ZmGH3.2* genes (Table S5). Overexpression of *ZmDREB2A* upregulated the expression of late embryogenesis abundant protein, whose products are thought to influence seed longevity positively (Qin *et al.*, 2007). Overall, ZmDREB2A enlists several pathways to safeguard seed longevity, situating it firmly as a hub positively influencing seed longevity.

Improving plant abiotic stress tolerance/seed aging tolerance without causing a growth penalty

Constitutive overexpression of *ZmDREB2A* enhanced plant abiotic stress tolerance; however, it causes a growth penalty under normal growth conditions (Sakuma *et al.*, 2006a; Gu *et al.*, 2016). The inducible expression of DREBs has been reported to enhance drought stress tolerance with limited effects on plant growth (Kasuga *et al.*, 1999; Wei *et al.*, 2016; Wei *et al.*, 2017). However, considering that the endogenous *DREBs* in the wild-type plants are also induced by drought stress, and yet wild-type plants are still vulnerable to this stress, the balance between the expression level boost of a TF gene such as *DREB* to the degree enabling enhanced drought stress tolerance without causing a noticeable growth penalty will be very complex.

Despite the extensive studies of the function and expression regulation of *DREB* genes, it has not been commercially applied in the production of genetic modified crops for improvement of crop abiotic stress tolerance. Gene editing technology has advanced quickly in recent years (Es *et al.*, 2019). The knowledge of the regulation of the IAA degradation and transduction pathway by the ZmDREB2A makes it practical to mutate specifically the DRE motif in the promoter of relevant genes in the IAA degradation/transduction pathway by gene editing technology in the future while simultaneously overexpressing *DREB* genes for improvement of the plant abiotic stress tolerance/seed aging tolerance without causing plant growth retardation.

ZmGOLS2 expression was upregulated by ZmDREB2A (Gu *et al.*, 2016). However, overexpression of the *ZmGOLS2* enhanced plant abiotic stress tolerance without causing a growth penalty under normal growth conditions (Gu *et al.*, 2016). These data suggest that it is feasible to improve crop abiotic stress tolerance through overexpressing a gene, such as *ZmGOLS2*, whose product executes a biochemically protective function, rather than overexpression of a TF gene, which controls many aspects of plant growth and abiotic stress tolerance.

In conclusion, ZmDREB2A negatively modulates seedling growth through stimulation of IAA degradation and signal transduction pathways while it positively regulates plant abiotic stress/seed aging tolerance through upregulation of raffinose biosynthesis. ZmDREB2A coordinates the balance between seedling growth and seed aging tolerance in maize (Figure 7). This finding reveals the molecular mechanism responsible for the retarded growth phenotype and the enhanced plant abiotic stress tolerance/seed aging tolerance of *DREB2A* overexpressing plants and thus contributes to the plant biotechnology field seeking to improve plant abiotic stress tolerance and seed aging tolerance without causing a yield penalty.

EXPERIMENTAL PROCEDURES

Characterization of Mu-inserted *zmdreb2a* mutant plants

Maize (*Zea mays*) inbred lines B73 and W22 were maintained in the lab. The *zmdreb2a* mutant seeds were obtained from the Maize Genetics Cooperation Stock Center from the UniformMu Transposon Resource (http://www.maizegdb.org/uniformmu) (Settles *et al.*, 2007). The UFMU07233 (*zmdreb2a-1*) and UFMU09182 (*zmdreb2a-2*) mutants (W22 background) were identified by searching the database using *ZmDREB2A* (GRMZM2G006745) as a query. The homozygous *zmdreb2a* mutants and their counterpart NS controls were obtained by self-pollination of the heterozygous mutants. The characterization of the mutants was performed by PCR using primers (F1a, F2a, R1a, R2a) and MU25 (Table S6). These primers were also used for the RT–PCR analysis of *ZmDREB2A* expression in the embryos of developing seeds.

Vector construction

The *GFP* or *ZmDREB2A* expression vectors used for maize protoplast transformation were constructed in previous studies (Gu *et al.*, 2016). Experimental dual luciferase reporter vectors in which the *Renilla* (*Renilla reniformis*) luciferase (*Rluc*) was controlled by either the *ZmGH3.2* promoter or the *ZmRAFS* promoter fragments, were constructed as follows. The different *ZmGH3.2* or *ZmRAFS* promoter fragments (depicted in Figure 4 or Figure 6) were amplified by PCR using primers (for *ZmGH3.2* fragment −264, use PF1 and PR1; −277, use PF2 and PR1; −277-C2, use PF3 and PR1; for *ZmRAFS* fragment −196, use PF4 and PR2; −208, use PF5 and PR2; −208-C2, use PF6 and PR2; Table S6) from B73 genomic DNA. The cloning of the PCR products followed a published method (Han *et al.*, 2020).

For construction of the *ZmGH3.2* bacterial expression vector, the *ZmGH3.2* open reading frame was amplified from cDNA synthesized from maize leaf RNA using primers 1F and 1R (Table S6). The *Bam*HI and *Hin*dIII restriction enzyme sites were designed in the primer to facilitate cloning. The amplicons were digested, gel purified and directionally ligated into the *pET-28a*(+) vector (TaKaRa, Kyoto, Japan).

Western blot

Polyclonal antibody against ZmDREB2A, ZmRAFS or ZmGH3.2 were prepared in the lab using a published method (Gu *et al.*, 2016; Li *et al.*, 2017b).

For comparison of the ZmDREB2A protein accumulation between *zmdreb2a* mutants and their NS controls by Western blot, the nuclear protein was extracted from the 35 DAP seed embryo. First, nuclei were isolated from 35 DAP seed embryos following a

© 2020 Society for Experimental Biology and John Wiley & Sons Ltd,

published method (Kodrzycki *et al.*, 1989). The nuclei were then resuspended in sodium dodecyl sulfate (SDS) lysis buffer (50 mM Tris–HCl, pH 8.0; 10 mM EDTA, pH 8.0; 1% SDS) and vibrated for 30 min at 4°C. The mixture was centrifuged at 13 000 ***g*** for 30 min at 4°C. The protein concentration of the supernatant was determined using the bicinchoninic acid method (Walker, 1994). In total, 50 μg protein was separated by SDS-polyacrylamide gel electrophoresis, transferred to membrane (Protran; Millipore, Burlington, Massachusetts, United States). Western blot analysis were performed following a published protocol (Gu *et al.*, 2016).

For Western blot characterization of the ZmGH3.2 or ZmRAFS protein accumulation in *zmdreb2a* mutants, soluble protein was extracted from the embryos of developing seeds at 35 DAP. Western blot characterization of ZmDREB2A, ZmGH3.2 or ZmRAFS protein accumulation in *ZmDREB2A* overexpressing protoplasts was performed following a published method (Han *et al.*, 2020).

AG treatment of seeds

Seeds were treated with high temperature and high moisture and then were evaluated for seed aging tolerance following a published protocol (Li *et al.*, 2017b). Three replications of 50 maize seeds each were tested for completion of germination. The number of seeds completing germination was counted every 24 h and the shoot/root length was measured 120 HAI. The photographs of NS and *zmdreb2a* seeds/seedlings were taken 120 HAI.

Quantification of hormones

The embryos were detached from mature, desiccated seeds of *zmdreb2a* mutants and their NS, and then were ground into powder in liquid nitrogen. The powders (120 mg) were extracted with 80% methanol at 4°C with vortexing once every 30 min for 12 h. The extract was centrifuged at 12 000 ***g*** at 4°C for 15 min. The supernatant was collected and then evaporated to dryness under a stream of nitrogen gas, reconstituted in 30% methanol. The solution was centrifuged and the supernatant was collected. The extracts were analyzed using an liquid chromatography (LC)-electrospray ionization (ESI)-tandem mass spectrometry (MS/MS) system (high-performance LC [HPLC], Shim-pack UFLC SHIMADZU CBM30A system; MS, Applied Biosystems 6500 Triple Quadrupole). The HPLC column was Waters ACQUITY UPLC HSS T3 C18 (1.8 μm, 2.1 mm × 100 mm); the solvent system was water (0.04% acetic acid)/acetonitrile (0.04% acetic acid); the gradient program was 95:5 v/v at 0 min, 5:95 v/v at 11.0 min, 5:95 v/v at 12.0 min, 95:5 v/v at 12.1 min, 95:5 v/v at 15.0 min; the flow rate was 0.35 ml/min; the temperature was 40°C; the injection volume was 5 μl. The effluent was alternatively connected to an ESI-triple quadrupole-linear ion trap (Q TRAP)-MS. The API 6500 Q TRAP LC/MS/MS System, equipped with an ESI Turbo Ion-Spray interface, was operated in a positive ion mode and controlled by Analyst 1.6 software (AB Sciex, Foster City, California, United States). The ESI source operation parameters were as follows: ion source, turbospray; source temperature, 500°C; ion spray voltage, 5500 V; curtain gas were set at 35.0 psi; the collision gas was medium. Declustering potential and collision energy for individual multiple reaction monitoring transitions was done with further declustering potential and collision energy optimization. A specific set of multiple reaction monitoring transitions were monitored for each period according to the plant hormones eluted within this period.

Exogenous IAA treatment of germinating seeds

For exogenous IAA treatment, seed germination was performed on filter paper soaked in different concentrations of IAA solutions in a plastic box at 28°C in darkness. The IAA solutions were replaced every 24 h. Three replications of 30 maize seeds each were tested. The number of seeds completing germination was counted every 24 h from 36 to 108 HAI. The shoot and root length were measured 120 HAI.

Maize protoplast transformation

Maize protoplast preparation and PEG-Ca^{2+}-mediated transformation followed a published protocol (Gu *et al.*, 2013). The protoplasts were incubated for another 17 h before being analyzed for RNA expression, protein accumulation and luciferase activity (Promega Inc., Madison, WI, USA).

RNA-Seq analysis

For RNA-Seq analysis of maize protoplast cells, maize B73 mesophyll protoplasts were transformed with either *GFP* or *ZmDREB2A* expression vector. The protoplasts were then incubated at 25°C for 17 h. The protoplasts were harvested and sent to the Beijing Genomics Institute for analysis using previously published protocols (Gu *et al.*, 2019). The differentially expressed genes in *ZmDREB2A* expressing maize protoplasts are provided in Table S1. For RNA-Seq analysis of maize seed embryo, maize *zmdreb2a-1* mutant and its NS control seeds were treated with or without AG treatment for 6 days following a published protocol (Li *et al.*, 2017b), the embryos were separated and sent to the Beijing Genomics Institute for analysis using previously published protocols (Gu *et al.*, 2019). Five embryos were combined to represent one biological replicate and there were three biological replicates.

RNA extraction, RT–PCR and real-time RT–PCR

RNA extraction, RT–PCR and real-time RT–PCR were performed following a published protocol (Li *et al.*, 2017b). Gene-specific primers were used for the detection of gene expression (*ZmDREB2A*: 2F and 2R; *ZmGH3.2*: 3F and 3R; *ZmRAFS*: 4F and 4R; *ZmDAO1*: 5F and 5R; *ZmIAA5*: 6F and 6R; *ZmIAA8*: 7F and 7R; *ZmIAA17*: 8F and 8R; *ZmIAA25*: 9F and 9R; *ZmIAA30*: 10F and 10R; and *ZmGAPDH*: 11F and 11R). All primers are listed in Table S6. For real-time RT–PCR analysis of mRNA expression of the *ZmDREB2A, ZmGH3.2* or *ZmRAFS* in developing embryos, the embryos were extracted from developing seeds at 21, 28 or 35 DAP. For real-time RT–PCR analysis of mRNA expression of the *ZmDREB2A, ZmGH3.2* or *ZmRAFS* in embryos of the imbibing seeds (the seeds were treated with or without AG treatment for 6 days; Li *et al.*, 2017b); the embryos were extracted from seeds during imbibition at 0, 24, 48 or 72 h. Two embryos were combined to represent one biological replicate and there were three biological replicates.

HPLC–evaporative light scattering detection of raffinose content

Soluble sugars were extracted with 80% ethanol from embryos that were separated from mature seeds. Soluble sugar content was detected and quantified by HPLC–evaporative light scattering detection as described previously (Li *et al.*, 2017b).

Preparation of GH3.2 protein for antibody and MBP-ZmDREB2A fusion protein and EMSA

The MBP-DREB2A fusion protein or MBP tag expression vector was constructed in a previous study (Gu *et al.*, 2016). The protein purification and EMSA were performed following a published method (Gu *et al.*, 2016). The double-stranded *GH3.2* promoter DNA, containing the identified *DRE* and its context sequence, was created by annealing

© 2020 Society for Experimental Biology and John Wiley & Sons Ltd,

two complementary oligonucleotides (ZmGH3.2 DRE-Sense and ZmGH3.2 DRE-Antisense; ZmRAFS DRE-Sense and ZmRAFS DRE-Antisense) following a published method (Gu *et al.*, 2016).

ChIP assay

The ChIP assay was performed following a published protocol (Han *et al.*, 2020) except that ZmDREB2A antibody was used to detect the ZmDREB2A binding to the DRE element in the promoter of the target gene *ZmGH3.2* or *ZmRAFS*. For PCR detection of the *ZmGH3.2* fragment, primers 12F and 12R were used; for PCR detection of the *ZmRAFS* fragment, primers 13F and 13R were used (Table S6). The IgG antibody was used as a control for ZmDREB2A antibody.

Measurement of 1000-grain weight

The 1000-seed weight was measured after harvesting and storage at 25 for at least 4 weeks. One cob was used as a replication, and at least four replications (cobs) were measured per genotype.

For water moisture content detection, the weight of detached embryos and endosperms was measured. The embryo and endosperm were dried at 105°C for 3 h in an oven before being dried at 70°C for 36 h to constant weight. The water moisture content was calculated as (fresh weight-dry weight)/fresh weight.

Statistical analysis

The data were analyzed by one-way ANOVA (Duncan test) or Student's *t*-test using IBM SPSS Statistics 19 (IBM Corp., Armonk, NY, USA).

ACCESSION NUMBERS

Sequence data can be found in Maize GDB under the following numbers: *ZmDREB2A* (GRMZM2G006745), *ZmGOLS1* (GRMZM2G165919), *ZmGOLS2* (GRMZM5G872256), *ZmRAFS* (GRMZM2G150906), *ZmDAO1* (GRMZM2G121700), *ZmGH3.2* (GRMZM2G378106), *ZmIAA5* (GRMZM2G004696), *ZmIAA8* (GRMZM2G167794), *ZmIAA17* (GRMZM2G030465), *ZmIAA25* (GRMZM2G115357), *ZmIAA30* (GRMZM2G001799), *ZmGAPDH* (GRMZM2G046804).

ACKNOWLEDGEMENTS

We acknowledge Dr. Hongchang Cui from Northwest A&F University for useful discussions about the manuscript. This research was funded by the National Key Research and Development Plan (2018YFD0100901) and the NSFC (31671776) to TZ. We wish to thank the Maize Genetics COOP Stock Center for providing the maize mutants and the Arabidopsis Biological Resource Center for the Arabidopsis mutants.

AUTHOR CONTRIBUTIONS

QH, KC, GH, JQ, CW and JG performed the research; LD and BD analyzed the data; and TZ, BD and JW conceived the experiments and wrote the article.

CONFLICT OF INTERESTS

The authors declare that they have no competing interests.

DATA AVAILABILITY STATEMENT

All relevant data can be found within the manuscript and its Supporting Information.

SUPPORTING INFORMATION

Additional Supporting Information may be found in the online version of this article.

Figure S1. Mutator interrupted *zmdreb2a-2* maize mutant (W22 background) showed lower seed aging tolerance and better seedling growth than its null segregant (NS-2) control.

Figure S2. Comparison of 1000-grain weight, plant stature and leaf appearance between the two *zmdreb2a* mutants and their null segregant controls.

Figure S3. Comparison of *ZmGH3.2* expression, IAA accumulation, between the *zmdreb2a-2* mutant and its NS-2 control.

Figure S4. Supplementation of IAA to the germinating seeds complemented the lower level IAA phenotype of NS-1 relative to the *zmdreb2a-1* mutant.

Figure S5. Supplementation of IAA to the germinating seeds complemented the lower level IAA phenotype of NS-2 relative to the *zmdreb2a-2* mutant.

Figure S6. The mRNA expression of relevant genes in the IAA degradation and transduction pathways was upregulated by *ZmDREB2A* overexpression in maize protoplasts.

Figure S7. Characterization of *ZmDREB2A*, *ZmGH3.2* or *ZmRAFS* mRNA accumulation in maize (W22) seed embryos during seed development and seed imbibition as determined by real time RT–PCR.

Figure S8. Comparison of *ZmRAFS* expression and raffinose accumulation between the *zmdreb2a-2* mutant and its NS-2 control.

Figure S9. Comparison of the upregulated genes by *ZmDREB2A* overexpression in *ZmDREB2A* overexpressing maize protoplast cells (OEDREB2A) relative to the *GFP* expressing cells, and the downregulated genes by knock down of the *ZmDREB2A* expression in *zmdreb2a-1* mutants seeds relative to the NS-1 seeds under AG6 treatment.

Table S2. Regulation of the expression of relevant genes involved in auxin biosynthesis, transport, degradation and signaling pathway by *ZmDREB2A* overexpression in maize protoplast cells (OEZmDREB2A) as determined by RNA-Seq.

Table S6. List of primers.

Table S1. Differentially expressed genes in maize protoplast between *ZmDREB2A* expressing cells and *GFP* expressing cells as determined by RNA-Seq (please refer to Excel file).

Table S3. Differentially expressed genes in maize embryo between seeds that were treated with accelerated aging (AG) and the seeds that were treated without AG (NAG) (please refer to Excel file).

Table S4. Downregulated genes in maize *zmdreb2a-1* mutant seed embryos as compared with that of NS-1 under accelerated aging (AG) treatment (please refer to Excel file).

Table S5. Genes that were upregulated by ZmDREB2A overexpression in *ZmDREB2A* overexpressing maize protoplasts, but were downregulated by knockdown of the *ZmDREB2A* expression in the *zmdreb2a-1* mutant seed embryo under AG6 treatment (please refer to Excel file).

REFERENCES

Angelovici, R., Galili, G., Fernie, A.R. and Fait, A. (2010) Seed desiccation: a bridge between maturation and germination. *Trends Plant Sci.* **15**, 211–218.

Ballesteros, D. and Walters, C. (2011) Detailed characterization of mechanical properties and molecular mobility within dry seed glasses: relevance to the physiology of dry biological systems. *Plant J.* **68**, 607–619.

Bernal-Lugo, I. and Leopold, A.C. (1992) Changes in soluble carbohydrates during seed storage. *Plant Physiol.* **98**, 1207–1210.

© 2020 Society for Experimental Biology and John Wiley & Sons Ltd,

Candat, A., Paszkiewicz, G., Neveu, M., Gautier, R., Logan, D.C., Avelange-Macherel, M.H. and Macherel, D. (2014) The Ubiquitous distribution of late embryogenesis abundant proteins across cell compartments in Arabidopsis offers tailored protection against abiotic stress. *Plant Cell*, **26**, 3148–3166.

Clerkx, E.J.M., Blankestijn-De Vries, H., Ruys, G.J., Groot, S.P.C. and Koornneef, M. (2003) Characterization of green seed, an enhancer of abi3-1 in Arabidopsis that affects seed longevity. *Plant Physiol.* **132**, 1077–1084.

Cramer, G.R., Urano, K., Delrot, S., Pezzotti, M. and Shinozaki, K. (2011) Effects of abiotic stress on plants: a systems biology perspective. *BMC Plant Biol.* **11**, 163.

Crowe, J.H., Carpenter, J.F. and Crowe, L.M. (1998) The role of vitrification in anhydrobiosis. *Annu. Rev. Physiol.* **60**, 73–103.

Dai, X., Mashiguchi, K., Chen, Q., Kasahara, H., Kamiya, Y., Ojha, S., DuBois, J., Ballou, D. and Zhao, Y. (2013) The biochemical mechanism of auxin biosynthesis by an arabidopsis YUCCA flavin-containing monooxygenase. *J. Biol. Chem.* **288**, 1448–1457.

Ding, X., Cao, Y., Huang, L., Zhao, J., Xu, C., Li, X. and Wang, S. (2008) Activation of the indole-3-acetic acid-amido synthetase GH3-8 suppresses expansin expression and promotes salicylate- and jasmonate-independent basal immunity in rice. *Plant Cell*, **20**, 228–240.

Downie, B. and Bewley, J.D. (2000) Soluble sugar content of white spruce (Picea glauca) seeds during and after germination. *Physiol. Plant.* **110**, 1–12.

Es, I., Gavahian, M., Marti-Quijal, F.J., Lorenzo, J.M., Khaneghah, A.M., Tsatsanis, C., Kampranis, S.C. and Barba, F.J. (2019) The application of the CRISPR-Cas9 genome editing machinery in food and agricultural science: Current status, future perspectives, and associated challenges. *Biotechnol. Adv.* **37**, 410–421.

Feng, S.G., Yue, R.Q., Tao, S., Yang, Y.J., Zhang, L., Xu, M.F., Wang, H.Z. and Shen, C.J. (2015) Genome-wide identification, expression analysis of auxin-responsive GH3 family genes in maize (Zea mays L.) under abiotic stresses. *J. Integr. Plant Biol.* **57**, 783–795.

Gangl, R. and Tenhaken, R. (2016) Raffinose Family oligosaccharides act as galactose stores in seeds and are required for rapid germination of Arabidopsis in the dark. *Front. Plant Sci.* **7**, 1115.

Gu, L., Han, Z., Zhang, L., Downie, B. and Zhao, T. (2013) Functional analysis of the 5′ regulatory region of the maize GALACTINOL SYNTHASE2 gene. *Plant Sci.* **213**, 38–45.

Gu, L., Jiang, T., Zhang, C., Li, X., Wang, C., Zhang, Y., Li, T., Dirk, L.M.A., Downie, A.B. and Zhao, T. (2019) Maize HSFA2 and HSBP2 antagonistically modulate raffinose biosynthesis and heat tolerance in Arabidopsis. *Plant J.* **100**, 128–142.

Gu, L., Zhang, Y., Zhang, M., Li, T., Dirk, L.M., Downie, B. and Zhao, T. (2016) ZmGOLS2, a target of transcription factor ZmDREB2A, offers similar protection against abiotic stress as ZmDREB2A. *Plant Mol. Biol.* **90**, 157–170.

Han, Q., Qi, J., Hao, G., Zhang, C., Wang, C., Dirk, L.M.A., Downie, A.B. and Zhao, T. (2020) ZmDREB1A Regulates RAFFINOSE SYNTHASE controlling raffinose accumulation and plant chilling stress tolerance in maize. *Plant Cell Physiol.* **61**, 331–341.

Higo, K., Ugawa, Y., Iwamoto, M. and Korenaga, T. (1999) Plant cis-acting regulatory DNA elements (PLACE) database: 1999. *Nucleic Acids Res.* **27**, 297–300.

Huot, B., Yao, J., Montgomery, B.L. and He, S.Y. (2014) Growth-defense tradeoffs in plants: a balancing act to optimize fitness. *Mol. Plant*, **7**, 1267–1287.

Jaglo-Ottosen, K.R., Gilmour, S.J., Zarka, D.G., Schabenberger, O. and Thomashow, M.F. (1998) Arabidopsis CBF1 overexpression induces COR genes and enhances freezing tolerance. *Science*, **280**, 104–106.

Kasuga, M., Liu, Q., Miura, S., Yamaguchi-Shinozaki, K. and Shinozaki, K. (1999) Improving plant drought, salt, and freezing tolerance by gene transfer of a single stress-inducible transcription factor. *Nat. Biotechnol.* **17**, 287–291.

Kasuga, M., Miura, S., Shinozaki, K. and Yamaguchi-Shinozaki, K. (2004) A combination of the Arabidopsis DREB1A gene and stress-inducible rd29A promoter improved drought- and low-temperature stress tolerance in tobacco by gene transfer. *Plant Cell Physiol.* **45**, 346–350.

Kodrzycki, R., Boston, R.S. and Larkins, B.A. (1989) The opaque-2 mutation of maize differentially reduces zein gene transcription. *Plant Cell*, **1**, 105–114.

Koster, K.L. and Leopold, A.C. (1988) Sugars and desiccation tolerance in seeds. *Plant Physiol.* **88**, 829–832.

Lang, S., Liu, X., Xue, H., Li, X. and Wang, X. (2017) Functional characterization of BnHSFA4a as a heat shock transcription factor in controlling the re-establishment of desiccation tolerance in seeds. *J. Exp. Bot.* **68**, 2361–2375.

Leprince, O., Harren, F.J.M., Buitink, J., Alberda, M. and Hoekstra, F.A. (2000) Metabolic dysfunction and unabated respiration precede the loss of membrane integrity during dehydration of germinating radicles. *Plant Physiol.* **122**, 597–608.

Leprince, O., Pellizzaro, A., Berriri, S. and Buitink, J. (2017) Late seed maturation: drying without dying. *J. Exp. Bot.* **68**, 827–841.

Leyser, O. (2018) Auxin signaling. *Plant Physiol.* **176**, 465–479.

Li, A.X., Zhou, M.Q., Wei, D.H., Chen, H., You, C.J. and Lin, J. (2017a) Transcriptome profiling reveals the negative regulation of multiple plant hormone signaling pathways elicited by overexpression of C-repeat binding factors. *Front. Plant Sci.* **8**, 1647.

Li, S., Zhao, Q., Zhu, D. and Yu, J. (2018) A DREB-Like transcription factor from maize (Zea mays), ZmDREB4.1, plays a negative role in plant growth and development. *Front. Plant Sci.* **9**, 395.

Li, T., Zhang, Y.M., Wang, D., Liu, Y., Dirk, L.M.A., Goodman, J., Downie, A.B., Wang, J.M., Wang, G.Y. and Zhao, T.Y. (2017b) Regulation of Seed Vigor by Manipulation of Raffinose Family Oligosaccharides in Maize and Arabidopsis thaliana. *Mol. Plant*, **10**, 1540–1555.

Liu, Q., Kasuga, M., Sakuma, Y., Abe, H., Miura, S., Yamaguchi-Shinozaki, K. and Shinozaki, K. (1998) Two transcription factors, DREB1 and DREB2, with an EREBP/AP2 DNA binding domain separate two cellular signal transduction pathways in drought- and low-temperature-responsive gene expression, respectively, in Arabidopsis. *Plant Cell*, **10**, 1391–1406.

Matthes, M.S., Best, N.B., Robil, J.M., Malcomber, S., Gallavotti, A. and McSteen, P. (2019) Auxin EvoDevo: Conservation and diversification of genes regulating auxin biosynthesis, transport, and signaling. *Mol. Plant*, **12**, 298–320.

Mellor, N., Band, L.R., Pencik, A. *et al.* (2016) Dynamic regulation of auxin oxidase and conjugating enzymes AtDAO1 and GH3 modulates auxin homeostasis. *Proc. Natl. Acad. Sci. USA*, **113**, 11022–11027.

Nakano, T., Suzuki, K., Fujimura, T. and Shinshi, H. (2006) Genome-wide analysis of the ERF gene family in Arabidopsis and rice. *Plant Physiol.* **140**, 411–432.

Nakashima, K., Shinwari, Z.K., Sakuma, Y., Seki, M., Miura, S., Shinozaki, K. and Yamaguchi-Shinozaki, K. (2000) Organization and expression of two Arabidopsis DREB2 genes encoding DRE-binding proteins involved in dehydration- and high-salinity-responsive gene expression. *Plant Mol. Biol.* **42**, 657–665.

Peterbauer, T., Mach, L., Mucha, J. and Richter, A. (2002) Functional expression of a cDNA encoding pea (*Pisum sativum* L.) raffinose synthase, partial purification of the enzyme from maturing seeds, and steady-state kinetic analysis of raffinose synthesis. *Planta*, **215**, 839–846.

Porco, S., Pencik, A., Rashed, A. *et al.* (2016) Dioxygenase-encoding AtDAO1 gene controls IAA oxidation and homeostasis in Arabidopsis. *Proc. Natl. Acad. Sci. USA*, **113**, 11016–11021.

Qin, F., Kakimoto, M., Sakuma, Y., Maruyama, K., Osakabe, Y., Tran, L.S., Shinozaki, K. and Yamaguchi-Shinozaki, K. (2007) Regulation and functional analysis of ZmDREB2A in response to drought and heat stresses in Zea mays L. *Plant J.* **50**, 54–69.

Sakuma, Y., Maruyama, K., Osakabe, Y., Qin, F., Seki, M., Shinozaki, K. and Yamaguchi-Shinozaki, K. (2006a) Functional analysis of an Arabidopsis transcription factor, DREB2A, involved in drought-responsive gene expression. *Plant Cell*, **18**, 1292–1309.

Sakuma, Y., Maruyama, K., Qin, F., Osakabe, Y., Shinozaki, K. and Yamaguchi-Shinozaki, K. (2006b) Dual function of an Arabidopsis transcription factor DREB2A in water-stress-responsive and heat-stress-responsive gene expression. *Proc. Natl. Acad. Sci. USA*, **103**, 18822–18827.

Sano, N., Rajjou, L., North, H.M., Debeaujon, I., Marion-Poll, A. and Seo, M. (2016) Staying alive: molecular aspects of seed longevity. *Plant Cell Physiol.* **57**, 660–674.

Saravitz, D.M., Pharr, D.M. and Carter, T.E. (1987) Galactinol synthase activity and soluble sugars in developing seeds of four soybean genotypes. *Plant Physiol.* **83**, 185–189.

Sehgal, A., Sita, K., Bhandari, K., Kumar, S., Kumar, J., Prasad, P.V.V., Siddique, K.H.M. and Nayyar, H. (2019) Influence of drought and heat stress, applied independently or in combination during seed development, on

© 2020 Society for Experimental Biology and John Wiley & Sons Ltd,

qualitative and quantitative aspects of seeds of lentil (Lens culinaris Medikus) genotypes, differing in drought sensitivity. *Plant Cell Environ.* **42**, 198–211.

Selvaraj, M.G., Ishizaki, T., Valencia, M. *et al.* (2017) Overexpression of an Arabidopsis thaliana galactinol synthase gene improves drought tolerance in transgenic rice and increased grain yield in the field. *Plant Biotechnol.* **15**, 1465–1477.

Settles, A.M., Holding, D.R., Tan, B.C. *et al.* (2007) Sequence-indexed mutations in maize using the UniformMu transposon-tagging population. *BMC Genom.* **8**, 116.

Shani, E., Salehin, M., Zhang, Y. *et al.* (2017) Plant stress tolerance requires Auxin-Sensitive Aux/IAA transcriptional repressors. *Curr. Biol.* **27**, 437–444.

Stepanova, A.N., Robertson-Hoyt, J., Yun, J., Benavente, L.M., Xie, D.Y., Dolezal, K., Schlereth, A., Jurgens, G. and Alonso, J.M. (2008) TAA1-mediated auxin biosynthesis is essential for hormone crosstalk and plant development. *Cell*, **133**, 177–191.

Stepanova, A.N., Yun, J., Robles, L.M., Novak, O., He, W., Guo, H., Ljung, K. and Alonso, J.M. (2011) The Arabidopsis YUCCA1 flavin monooxygenase functions in the indole-3-pyruvic acid branch of auxin biosynthesis. *Plant Cell*, **23**, 3961–3973.

Stockinger, E.J., Gilmour, S.J. and Thomashow, M.F. (1997) Arabidopsis thaliana CBF1 encodes an AP2 domain-containing transcriptional activator that binds to the C-repeat/DRE, a cis-acting DNA regulatory element that stimulates transcription in response to low temperature and water deficit. *Proc. Natl. Acad. Sci. USA*, **94**, 1035–1040.

Taji, T., Ohsumi, C., Iuchi, S., Seki, M., Kasuga, M., Kobayashi, M., Yamaguchi-Shinozaki, K. and Shinozaki, K. (2002) Important roles of drought- and cold-inducible genes for galactinol synthase in stress tolerance in Arabidopsis thaliana. *Plant J.* **29**, 417–426.

Tao, Y., Ferrer, J.L., Ljung, K. *et al.* (2008) Rapid synthesis of auxin via a new tryptophan-dependent pathway is required for shade avoidance in plants. *Cell*, **133**, 164–176.

van Zanten, M., Koini, M.A., Geyer, R., Liu, Y.X., Brambilla, V., Bartels, D., Koornneef, M., Fransz, P. and Soppe, W.J.J. (2011) Seed maturation in Arabidopsis thaliana is characterized by nuclear size reduction and increased chromatin condensation. *Proc. Natl. Acad. Sci. USA*, **108**, 20219–20224.

Walker, J.M. (1994) The bicinchoninic acid (BCA) assay for protein quantitation. *Methods in Mol. Biol.* **32**, 5–8.

Wang, P.C., Zhao, Y., Li, Z.P. *et al.* (2018) Reciprocal regulation of the TOR kinase and ABA receptor balances plant growth and stress response. *Mol. Cell*, **69**, 100–112.

Wei, T., Deng, K., Liu, D. *et al.* (2016) Ectopic expression of DREB transcription factor, AtDREB1A, confers tolerance to drought in transgenic salvia miltiorrhiza. *Plant Cell Physiol.* **57**, 1593–1609.

Wei, T., Deng, K., Zhang, Q. *et al.* (2017) Modulating AtDREB1C expression improves drought tolerance in salvia miltiorrhiza. *Front. Plant Sci.* **8**, 52.

Yamaguchi-Shinozaki, K. and Shinozaki, K. (1994) A novel cis-acting element in an Arabidopsis gene is involved in responsiveness to drought, low-temperature, or high-salt stress. *Plant Cell*, **6**, 251–264.

Yoshida, T., Mogami, J. and Yamaguchi-Shinozaki, K. (2014) ABA-dependent and ABA-independent signaling in response to osmotic stress in plants. *Curr. Opin. Plant Biol.* **21**, 133–139.

Zhang, J., Lin, J.E., Harris, C., Campos Mastrotti Pereira, F., Wu, F., Blakeslee, J.J. and Peer, W.A. (2016) DAO1 catalyzes temporal and tissue-specific oxidative inactivation of auxin in Arabidopsis thaliana. *Proc. Natl. Acad. Sci. USA*, **113**, 11010–11015.

Zhang, Y., Sun, Q., Zhang, C., Hao, G., Wang, C., Dirk, L.M.A., Downie, A.B. and Zhao, T. (2019) Maize VIVIPAROUS1 interacts with ABA INSENSITIVE5 to regulate GALACTINOL SYNTHASE2 expression controlling seed raffinose accumulation. *J. Agri. Food Chem.* **67**, 4214–4223.

Zhu, J.K. (2016) Abiotic stress signaling and responses in plants. *Cell*, **167**, 313–324.

© 2020 Society for Experimental Biology and John Wiley & Sons Ltd,